

STUDY OF THE DP-ELASTIC SCATTERING AT 2 GEV

A.A. Terekhin^{*†}, Yu.V. Gurchin^{*}, A.Yu. Isupov^{*}, A.N. Khrenov^{*},
 A.K. Kurilkin^{*}, P.K. Kurilkin^{*}, V.P. Ladygin^{*}, N.B. Ladygina^{*},
 S.M. Piyadin^{*}, S.G. Reznikov^{*}, I.E. Vnukov^{**}.

^{*}*LHEP-JINR, 141980, Dubna, Moscow region, Russia*

^{**}*BelSU, 308015, Belgorod, Russia*

[†]*E-mail: aterekhin@jinr.ru*

Abstract

The results on the measurements of dp -elastic scattering cross section at the energy 2 GeV at Internal Target Station at the Nuclotron JINR are reported. The data were obtained for the angular range of $70^\circ - 107^\circ$ in the c.m.s. by using CH_2 and C targets. The results are compared with the existing data and with the theoretical calculations based on the relativistic multiple scattering theory.

Introduction

The dp -elastic scattering reaction is the longtime subject of the theoretical and experimental investigations. Many experiments were performed by using the different targets and the accelerated particles beams. Today, there are quite extensive experimental material. Also now the different theoretical models are developed to describe of data at the different energies: the Faddeev calculations in the momentum space [1] and configuration space [2], and variational calculations based on the solution of the three-particle Schroedinger equation [3–5]. The momentum- space Faddeev equations for three-nucleon scattering can now be solved with high accuracy for the most modern two- and three-nucleon forces below 200 MeV/n of the projectile energy [6, 7]. The discrepancy between the theory and experiment is increasing with the energy increasing indicating the possibility of relativistic effects. The theoretical calculations using not only 2N forces but also different 3N forces [8, 9] give the best agreement with experimental data.

The experimental material for dp -elastic scattering covers the energy range from tens to thousands MeV/n. The precise data were obtained at RIKEN at the energies of 70, 100 and 135 MeV/n [10] for the angular range of $10^\circ < \theta^* < 180^\circ$. The analogous experiment was performed in RCNP at the energy of 250 MeV/n [11], where the data on the cross section and complete set of proton spin observables were obtained. The goal of these experiments was to study the 3NF contribution and to test modern models of the three-nucleon forces.

The differential cross section data at energies 470 and 590 MeV/n in the backward hemisphere were obtained at the National Aeronautics and Administration Space Radiation Effects Laboratory [12]. The absolute differential cross section was measured at 641.3 and 792.7 MeV/n in the angular range of $35^\circ - 115^\circ$ and $35^\circ - 140^\circ$, respectively [13]. The results can be fit with a relativistic multiple-scattering theory which uses off-mass-shell extrapolations of the nucleon-nucleon amplitudes suggested by the structure of derivative meson-nucleon couplings [14]. Relativistic-impulse-approximation calculations do not describe these data [15]. The data were obtained at the Brookhaven National Laboratory (BNL) at 1 GeV/n for the angles of $10^\circ < \theta^* < 170^\circ$ [16]. The new data on the differential cross section of the dp -elastic scattering at 1.25 GeV/n were obtained with HADES

detector [17]. The experimental data are described by the relativistic multiple scattering theory which takes both single and double interactions into account [18].

The transition to higher energies (few hundred MeV/n and higher) will allow one to understand the mechanism of manifestation of the fundamental degrees of freedom at distances of the order of the nucleon size. Glauber scattering theory which takes both single and double interactions in this case is a classic approach [19, 20].

The purpose of DSS (Deuteron Spin Structure) project [21] is the broadening of the energy and angular ranges of measurement of different observables in processes including 3-nucleon systems. The experiments to study of the dp -elastic scattering at Internal Target Station (ITS) [22] at the Nuclotron in the range from 150 to 1000 MeV/n are performed in the frame of this project. The experimental setup allows one to obtain the different observables from 60° to 140° in the c.m.s. The new preliminary differential cross section data were obtained at ITS Nuclotron at the energies from 250 to 440 MeV/n [23]. Recently, the deuteron vector and tensor analyzing powers have been obtained at 440 MeV/n [24]. The angular dependence of the differential cross section obtained at 2GeV is presented in this paper. The results are compared with the existing data [25] and [16] and with the theoretical calculations based on the relativistic multiple scattering theory [18].

1 Experiment

The measurements were performed at ITS [22] at the Nuclotron JINR by using $10\mu\text{m}$ CH_2 and $8\mu\text{m}$ C targets. New ITS DAQ system was used during the data taking [26]. The elastically-scattered deuterons and protons were counted by two pairs of detectors placed symmetrically with respect to the beam direction. This allows one to improve the quality of the experiment. During the methodical measurements all deuteron- and proton-counters (the description of which can be found in [27]) are based on the FEU-85. During the main measurements these detectors were replaced to the counters based on the Hamamatsu H7416MOD previously used in the experiment [24]. Another two detectors (PP-detectors) based on the FEU-85 and FEU-63 were used to count the quasi-elastically scattered protons. Each of such a counter consists of the ΔE and E - detectors [28]. The layout of the counters with respect to the beam direction is shown in Fig.1. The $D_{1,2}$, $P_{1,2}$ and $PP_{1,2}$ are deuteron-, proton- and PP-detectors, respectively. All the counters were placed in horizontal plane. The DP-detectors were rotated to give an angular range of the $\theta_{lab} = 19^\circ$ to 50° ($\theta_{c.m.} = 70^\circ$ to 120°). The precision of the detectors mount is 0.3° in the laboratory system, which corresponds to 0.6° in the c.m.s. The PP-detectors were mounted at the angle corresponding to quasi-elastic scattering at $\theta_{c.m.} = 90^\circ$ and remained stationary throughout the experiment. These detectors were used as relative luminosity monitors. The sizes of the P-, D- and PP- counters are $20 \times 60 \times 20 \text{ mm}^3$, $50 \times 50 \times 20 \text{ mm}^3$ and $\phi 100 \times 200 \text{ mm}^3$, respectively. The distances from proton-, deuteron- and monitor- counters to the point of the beam interaction with the target are 60, 56 and 100 cm, respectively. The angular spans of P-, D- and PP- detectors were 2° , 5° , 10° in the laboratory system, which corresponds to 4° , 10° and 20° in the c.m.s., respectively. The characteristics of the detectors are shown in Table 1.

The VME based data acquisition system was used for the data taking from scintillation detectors. TQDC16 module [29] allows one to measure the amplitude and time appearance of the signal simultaneously. Each module is separated into two parts with 8 input

Detectors	Size, mm ³	Distance from target, cm	Angular span, deg	
			Lab. sys.	c.m.s.
P	20×60×20	60	2	4
D	50×50×20	56	5	10
PP	φ100×200	100	10	20

Table 1. The characteristics of the detectors.

channels having own first level trigger logics. In the current experiment the first level trigger signal was appeared when the signal from one module part coincides with the signal from any channel of other part.

The methodical measurements by using the scintillation counters based on the FEU-85 were performed. The DP- and monitor- detectors were mounted at angles $\theta_{c.m.} = 75^\circ$ and $\theta_{c.m.} = 90^\circ$ in the c.m.s., respectively. The analysis of subtraction of the time signal taken from the deuteron- and proton- detectors showed that the dp -elastic scattering events and background cannot be selected [30]. Therefore, the scintillation counters based on the Hamamatsu were used for the current measurements.

The results of measurements are shown in Fig.2. One can see that the use of Hamamatsu photomultipliers allow selecting the dp -elastic scattering events and background from carbon.

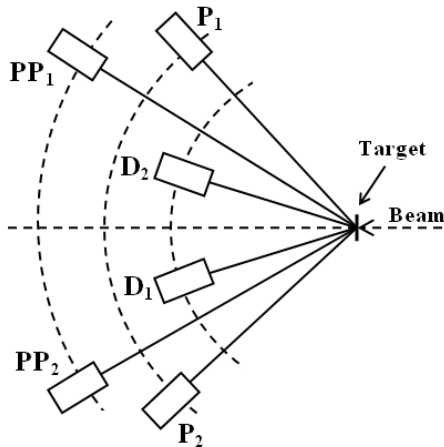


Figure 1: Layout of the counters with respect to the beam direction. D_{1,2}, P_{1,2}- deuteron and proton detectors, PP_{1,2}- the relative luminosity monitors.

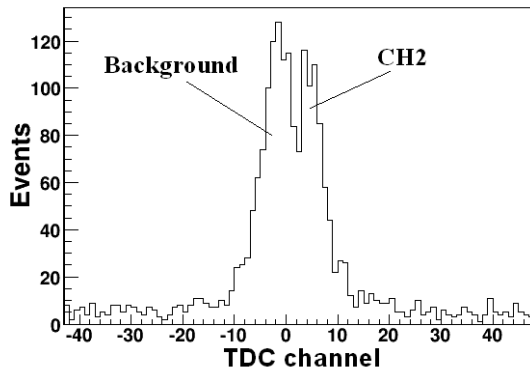


Figure 2: The subtraction of the timing signal from deuteron- and proton- counters for $\theta_{c.m.} = 70^\circ$ in the c.m.s.. The data were obtained by using the counters based on the Hamamatsu H7416MOD.

2 Data analysis

The data analysis was performed in the following way. Firstly, the identity of detectors work of each pair was tested. The target is moved by using a stepping motor. The correlation of motor pulse and time appearance of triggers are shown in Fig.3. The smooth line corresponds to the time when the target is located in the beam. The time range after 1800 msec corresponds to the case when the target is removed from the beam. The acquisition time of triggers has been divided into the consecutive interval. The value of the each interval equal to 200 ms. The reconstructed events ("true" triggers) for DP-detectors are defined as the coincidence of signals from the one proton-counter with the corresponding D-counter. For monitor counters the reconstructed events are defined as the coincidence of both ΔE and E detectors. The ratio of signal coincidences of D₁- and P₁- counters to signal coincidences of D₂- and P₂- counters was made for the each interval. The dependence of the value $R = N_1/N_2$ from the time interval, where $N_{1(2)}$ - the number of coincidences of P₁₍₂₎- and D₁₍₂₎- detectors counts, is shown in Fig. 4. One can see, that the value of the ratio is ≈ 1 in the domain when the target is within the beam. The similar results were obtained for the PP₁₍₂₎ detectors. This demonstrates small geometrical misalignment of the experimental setup with respect to the beam direction.

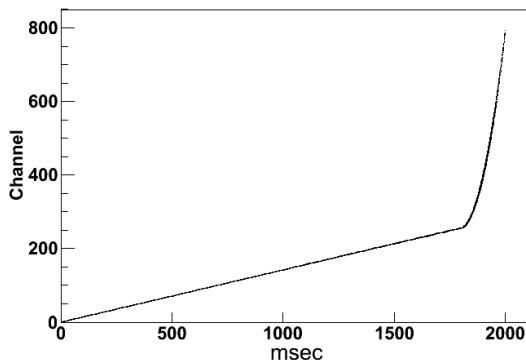


Figure 3: The correlation of motor pulse and time appearance of triggers.

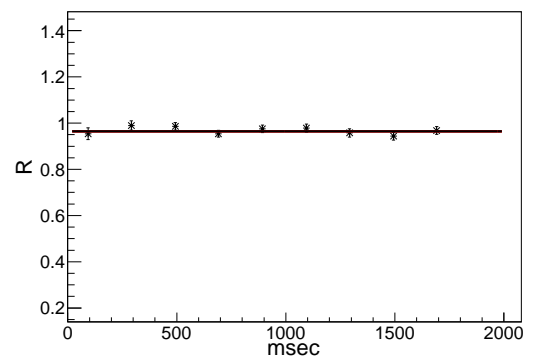


Figure 4: The ratio of signal coincidences of D₁- and P₁- counters to signal coincidences of D₂- and P₂- counters for $\theta_{c.m.} = 100^\circ$ in the c.m.s. as a function of the acquisition time of triggers.

The procedure to obtain differential cross section data was made by analysis of the amplitude spectra. The graphical cut was imposed on the signal amplitudes correlation for D- and P- detectors to select dp -elastic scattering particles (Fig. 5).

The estimation of the background in the amplitude data was performed by using the temporary gates on the deuteron and proton time difference spectra. The subtraction of the timing signal from deuteron- and proton- counters was made by using the cut for signal amplitudes correlation (Fig 6). In this distribution the dp -elastic scattering events (I domain) and the background (II and III domains) are selected so that the width of both domains are equal.

The amplitude distribution for proton counter by using these timing gates is shown in Fig. 7 A. The subtraction of the resulting spectra allows reducing of the background (Fig. 7 B).

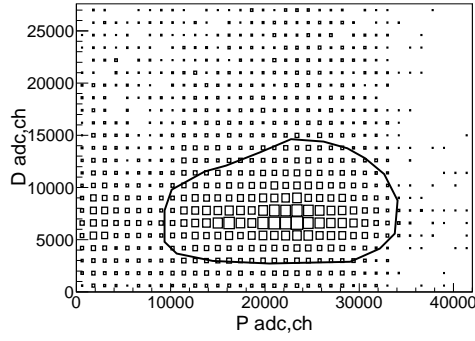


Figure 5: The signal amplitudes correlation for deuteron- and proton detectors. The solid line is the graphical cut to select dp -elastic scattering events.

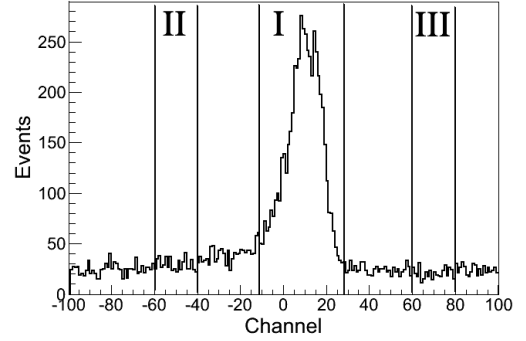


Figure 6: The time difference of signals arrival from the deuteron and proton counters for $\theta_{c.m.} = 70^\circ$ in the c.m.s.

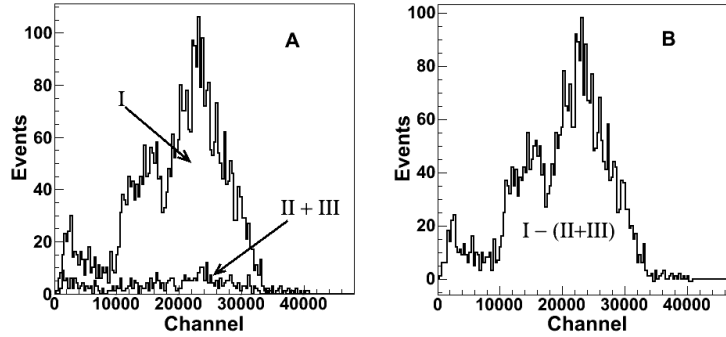


Figure 7: The background subtraction procedure for the amplitude spectrum of proton counter for $\theta_{c.m.} = 70^\circ$ in the c.m.s..

The above analysis corresponds to the data obtained using CH_2 -target. Analogous procedure was performed for the case with the C-target.

The next stage is the CH_2 -C subtraction procedure. The carbon background subtraction normalization coefficient k is deduced from the interval $a_{min} < a < a_{max}$, where a - channels of CH_2 - and C-amplitude distributions:

$$k = \frac{N_{\text{CH}_2}|_{a_{min} < a < a_{max}}}{N_C|_{a_{min} < a < a_{max}}}. \quad (1)$$

Here N_{CH_2} and N_C - CH_2 - and C-amplitude distributions integrals in a -interval within the window shown in Fig. 8 A by the solid lines. The carbon background can be then subtracted as:

$$N_{dp} = N_{\text{CH}_2} - kN_C, \quad (2)$$

where N_{dp} is the resulting dp -elastic scattering distribution, N_{CH_2} is the total CH_2 -distribution, kN_C is the normalized C-distribution within the window shown in Fig. 8 B by the dotted lines.

In Fig.8 A the CH_2 -distribution is shown by the solid line. The normalized C-spectrum is shown by the dotted line. In Fig.8 B the result of subtraction is demonstrated. Such procedure was performed for proton amplitude spectra for each $\theta_{c.m.}$.

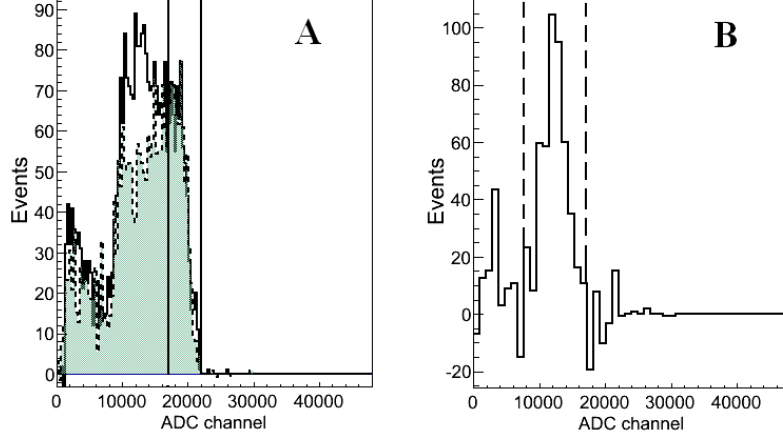


Figure 8: The procedure of $CH_2 - C$ subtraction for $\theta_{c.m.} = 70^\circ$ in the c.m.s. A - is the CH_2 - and normalized C- distributions given by the solid and dotted histograms, respectively, vertical solid lines - is the interval of the normalization. B - is the result of $CH_2 - C$ subtraction, vertical dashed lines are the gates indicating the domain of the dp -elastic scattering events.

3 Results and discussions

The cross section was calculated using normalization to world data [16] at $\theta_{c.m.} = 70^\circ$ having the value $(d\sigma/d\Omega)|_{70^\circ} = 0.024 \pm 0.002$ mb/sr:

$$\left(\frac{d\sigma}{d\Omega}\right)_{c.m.} = \frac{N_{dp}}{\Delta\Omega_{lab}^{dp}} \frac{C_{norm}}{N_M} J. \quad (3)$$

Here N_{dp} - is the number of dp -elastic scattering events (after proper background subtraction), $\Delta\Omega_{lab}^{dp}$ - the effective angular span of proton detectors in the laboratory system, N_M - is the number reconstructed events from one of the PP-counters, C_{norm} - is the normalization coefficient, obtained at 70° c.m.s.

The transition from lab to the c.m. frame for differential cross section takes place by the transformation jacobian J which can be obtained by the kinematic calculations as:

$$J = \frac{d\cos\theta_{lab}}{d\cos\theta_{c.m.}}. \quad (4)$$

The effective angular span of proton detectors was calculated with the Pluto simulation package [32]. The value of the $d\Omega_{lab}$ decreases with the increasing of the $\theta_{c.m.}$.

The statistical error associated with the background subtraction (eq. (2)) is roughly given by $\delta N_{dp}^{stat} = \sqrt{N_{CH_2} + k^2 N_C}$. The systematic error is due to normalization and $CH_2 - C$ subtraction procedure. The latter is defined as $\delta N_{dp}^{sys} = \delta k N_C$. The mean

value of $\delta k \approx 5\%$. In general, the uncertainty of the normalization coefficient C can be expressed from eq. 3 as:

$$\delta C_{norm} = C \sqrt{\left(\frac{\delta\sigma}{\sigma}\right)^2 + \left(\frac{\delta N_M}{N_M}\right)^2 + \left(\frac{\delta N_{dp}^{stat}}{N_{dp}}\right)^2 + \left(\frac{\delta N_{dp}^{sys}}{N_{dp}}\right)^2}. \quad (5)$$

Here all values are defined for the $\theta_{c.m.} = 70^\circ$. $\delta\sigma/\sigma$ - is the differential cross section relative error which equal about 8% [16]. The value $\delta N_M/N_M$ is negligible. In particular, the uncertainty of normalization for the data for the $\theta_{c.m.} = 70^\circ$ is determined by the first and fourth term only. The total systematic error varies in the range from 17% to 40%.

The theoretical predictions for the differential cross section have been obtained in the relativistic multiple-scattering theory frame [18]. In this model the reaction amplitude is defined by the corresponding transition operator. This operator obeys the Alt-Grassberger-Sandhas (AGS) equation [33, 34]. After iteration these equations up to second-order term over NN t -matrix the reaction amplitude is defined as a sum of the three terms, which correspond to one-nucleon exchange (*ONE*), single scattering (*SS*) and double scattering (*DS*) reaction mechanisms. Since the ONE term gives a considerable contribution only at backward angles, this term was not included into consideration. Thus, the reaction amplitude is defined as a sum of two terms only. Diagrams for *SS* and *DS* are presented in Fig. 9. All calculations were performed with the CD Bonn deuteron wave function [35]. The parameterization of the NN t -matrix was based on the use of the modern phase shift analysis [36] results.

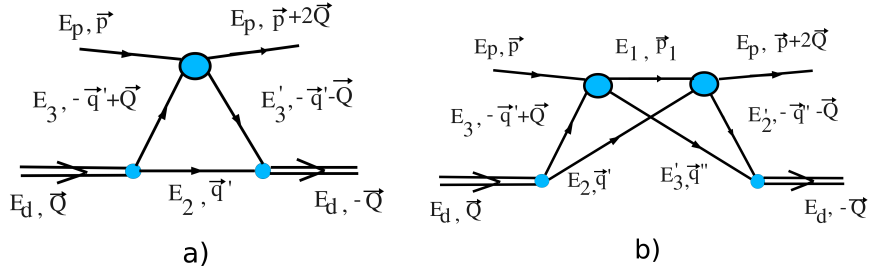


Figure 9: The diagrams taken into consideration for the calculations within relativistic multiple-scattering model [18]: a) - single scattering, b) - double scattering.

In Fig.10 the data for differential cross section at 2 GeV are compared with the world data and with the theoretical predictions. The new data are shown by the solid squares. The errors are the statistical only. The systematic errors are shown by the solid gray band. The data obtained earlier for forward angles [25] are shown by the solid circles. The open triangles are world data from [16] obtained with a monochromatic protons beam at the Brookhaven Cosmotron by using a liquid-deuterium target. The dashed and solid lines are the calculations without and with *DS* term, respectively. One can see that the new data at $\theta_{c.m.} \leq 90^\circ$ are in good agreement with the world data. The discrepancy is increased at large angles, nevertheless, the data are in agreement with the errors which increase with the angle increasing. On the other hand, there is better agreement with theoretical calculations taking into account DS at these angles.

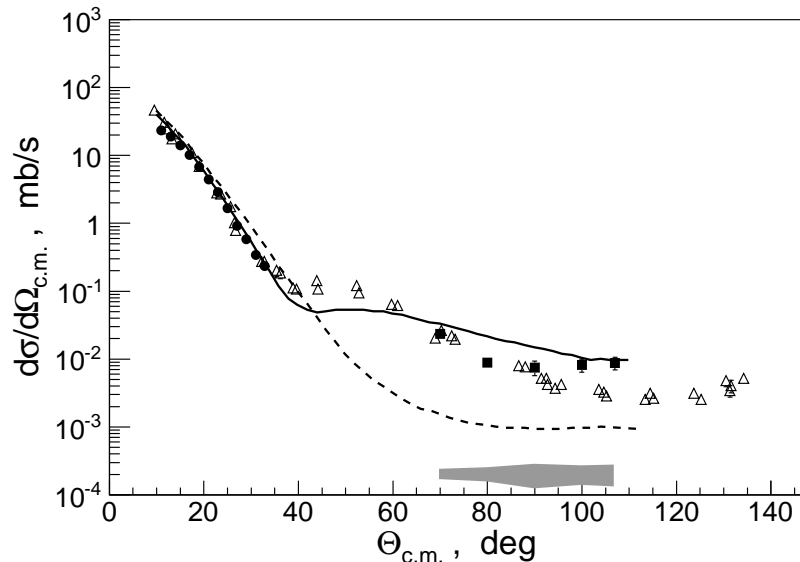


Figure 10: The differential cross section for dp -elastic scattering at 1000 MeV/n. Squares - the results of this work, solid band - the systematic errors, circles - data from [25], triangles - data from [16]. The dashed and solid lines are the calculations without and with DS term, respectively.

Fig. 10 shows that the single scattering mechanism does not reproduce the experimental data at the scattering angles θ^* larger than 45° . The inclusion of the double scattering term in the calculations provides better agreement with the experimental results. However, some discrepancy remains. Probably, taking into account new reaction mechanisms like explicit Δ -isobar excitation will improve the description of the data.

Conclusion

The procedure to obtain differential cross section in dp -elastic scattering is shown. In the experiment the deuteron beam at energy 2 GeV, the CH_2 - and C- targets were used. The data analysis was performed by using the CH_2 - C subtraction for amplitude spectra of proton detectors.

The differential cross section data are obtained for the angular range of $70^\circ - 107^\circ$ in the c.m.s. The results were compared with the data obtained early at the Synchrophasotron [25] and the world data obtained at the Brookhaven Cosmotron [16]. The shape of the angular dependence of the relatively normalized data obtained at the Nuclotron agrees with the behaviour of the previously obtained data [16]. The discrepancy is increased at large angles, but nonetheless data are in agreement with achieved experimental accuracy.

The data are compared with the calculations performed within the framework of the relativistic multiple scattering theory [18]. It is shown that taking into account the double scattering term improves the description of the obtained experimental results.

The work has been supported in part by the RFBR grant 13-02-00101a.

References

- [1] *H. Witala, Th.Cornelius, W.Glockle* Elastic scattering and break-up processes in then-d system // *Few-Body Systems*. **3**, 1988. P.123.
- [2] *J.L. Friar, et al.* Benchmark solutions for n-d breakup amplitudes. // *Phys.Rev.* **C51**, 1995. P. 2356.
- [3] *A. Kievsky, M.Viviani, S.Rosati* Polarization observables in p - d scattering below 30-MeV // *Phys.Rev.* **C64**, 2001. 024002.
- [4] *M. Viviani, A.Kievsky, S.Rosati* The Kohn variational principle for elastic proton-deuteron scattering above deuteron breakup threshold // *Few-Body Syst.* **30**, 2001. P.39.
- [5] *A. Deltuva et al.* Benchmark calculation for proton-deuteron elastic scattering observables including Coulomb // *Phys.Rev.* **C71**, 2005. 064003.
- [6] *W. Glockle et al.* The three-nucleon continuum: achievements, challenges and applications // *Phys.Rep.* **274**, 1996. P.107.
- [7] *J. Kuros-Zolnierczuk, H.Witala et al.* Three-Nucleon Force Effects in Nucleon Induced Deuteron Breakup: Comparison to Data (II) // *Phys.Rev.* **C66**, 2002. 024004.
- [8] *S.A. Coon, H.K.Han* Revorking the Tucson-Melbourne Three-Nucleon Potential // *Few-Body Systems* **30**, 2001. P.131.
- [9] *B.S. Rudliner et al.* Quantum Monte Carlo calculations of nuclei with $A \leq 7$ // *Phys. Rev.* **C56**, 1997. P. 1720.
- [10] *K. Sekiguchi et al.* Complete set of precise deuteron analyzing powers at intermediate energies: Comparison with modern nuclear force predictions // *Phys. Rev.* **C65**, 2002. 034003.
- [11] *K. Hatanaka et al.* Cross section and complete set of proton spin observables in pd elastic scattering at 250MeV // *Phys.Rev.* **C66**, 2002. 044002.
- [12] *J.C. Alder et al.* Elastic pd scattering at 316,364,470 and 590 MeV in the Backward Hemisphere // *Phys. Rev.* **C6 6**, 1972. P.2010.
- [13] *E. Culmez et al.* Absolute differential cross section measurements for proton-deuteron elastic scattering at 641.3 and 792.7 MeV // *Phys. Rev.* **C43 5**, 1991. P.2067.
- [14] *E.Bleszynski et al.* Spin Observables In Proton Deuteron Elastic Scattering // *AIP Conf.* **150**, 1986. P.1208.
- [15] *J.R. Shepard et al.* Relativistic Impulse Approximation For P Nucleus Elastic Scattering // *Phys.Rev.Lett.* **50**, 1983. P.1443-1446.
- [16] *G.W. Bennet et al.* Proton-deuteron scattering at 1 BeV // *Phys. Rev. Lett.* **19**, 1967. P.387.

- [17] *P.K. Kurilkin et al.* New data on the differential cross section of the dp -elastic scattering at 2.5 GeV obtained with HADES detector // PoS Baldin-ISHEPP-XXI 040 2012;
The dp -elastic cross section measurement at the deuteron kinetic energy of 2.5-GeV // Eur. Phys. J. Web Conf. **37**, 2012. 09021.
- [18] *N.B. Ladygina et al.* Differential Cross Section of DP-Elastic Scattering at Intermediate Energies // Eur. Phys. J. **A42**, 2009. P.91.
- [19] *V. Franco, R.J.Glauber* Small-Angle High-Energy Scattering by Deuterons // Phys. Rev. Lett. **16**, 1966. P.944.
- [20] *V. Franco, E.Coleman* Double Scattering in High-Energy Elastic Collisions with Deuterons // Phys.Rev.Lett. **17**, 1966. P.827.
- [21] *V.P. Ladygin et al.* Short-range correlation studies in collisions of polarized nuclei at Nuclotron-M // Eur. Phys. J. Web of Conf. **3**, 2010. 04004;
Few-body studies at Nuclotron-JINR // Few Body Syst. **55**, 2014. 709.
- [22] *Malakhov A.I. et al.* Potentialities of the internal target station at the Nuclotron. Nucl. Instrum. Methods // Phys. Res. **A440**, 2000. P.320329.
- [23] *Yu.V. Gurchin et al.* The differential cross-section on dp -elastic scattering at 400-880 MeV obtained at Nuclotron // Nucl.Phys.Proc.Suppl. **245**, 2013. P.271-274;
The cross-section in dp -elastic scattering at the energies of 500-MeV, 700-MeV and 880-MeV obtained at the internal target station of nuclotron // Phys.Part.Nucl.Lett. **10**, 2013. P.243-247.
- [24] *P.K. Kurilkin et al.* Measurement of the vector and tensor analyzing powers for dp -elastic scattering at 880 MeV // Phys. Lett. **B715**, 2012. P.61-65.
- [25] *V.V. Glagolev et al.* Measurement of the differential cross-section and deuteron vector analyzing power in dp -elastic scattering at 2.0-GeV // Eur. Phys. J. **A48**, 2012. P.182.
- [26] *A.Yu. Isupov et al.* The Nuclotron internal target control and data acquisition system // Nucl. Instrum. Methods Phys. Res. **A698**, 2013. P.127134.
- [27] *Gurchin Yu.V. et al.* Detection equipment for investigating dp -elastic scattering at internal target of Nuclotron in the framework of DSS project. // Phys. Part. Nucl. Lett. **8**, 2011. P.950958.
- [28] *S.M. Piyadin et al.* The study of the $dp \rightarrow ppn$ reaction at 500-MeV of the deuteron energy at ITS nuclotron // Nucl.Phys.Proc.Suppl. **219-220**, 2011. P.251.
- [29] <http://afi.jinr.ru/TQDC-16>
- [30] *A.A. Terekhin et al.* Preparation of experiments to study light nuclei structure at Nuclotron // PoS Baldin-ISHEPP-XXI 2012. 005
- [31] <http://gwdac.phys.gwu.edu/analysis/nn-analysis>;
D. Albers et al. A precision measurement of pp elastic scattering cross-sections at intermediate energies // Eur. Phys. J. **A22**, 2004. P.125-148.

- [32] *I. Froehlich et al.* A versatile method for simulating $pp \rightarrow ppe^+e^-$ and $dp \rightarrow pne^+e^-p(\text{spec})$ reactions // Eur.Phys.J. **A45** 2010. P.401-411.
- [33] *E.O. Alt et al.* Reduction of the three-particle collision problem to multi-channel two-particle lippmann-schwinger equations // Nucl.Phys. **B2** 1967. P.167.
- [34] *E.W. Schmid, H. Ziegelmann* The Quantum Mechanical Three-Body Problem // Oxford, Pergamon Press, 1974.
- [35] *R.Machleidt* The High precision, charge dependent Bonn nucleon-nucleon potential (CD-Bonn) // Phys.Rev. **C63**, 2001. 024001.
- [36] <http://gwdac.phys.gwu.edu>.

This figure "1_scheme1.jpg" is available in "jpg" format from:

<http://arxiv.org/ps/1503.07968v1>

This figure "10_s2000.jpg" is available in "jpg" format from:

<http://arxiv.org/ps/1503.07968v1>

This figure "2_tdc.jpg" is available in "jpg" format from:

<http://arxiv.org/ps/1503.07968v1>

This figure "3_timestamp_100.jpg" is available in "jpg" format from:

<http://arxiv.org/ps/1503.07968v1>

This figure "4_R.jpg" is available in "jpg" format from:

<http://arxiv.org/ps/1503.07968v1>

This figure "5_adc_cut.jpg" is available in "jpg" format from:

<http://arxiv.org/ps/1503.07968v1>

This figure "6_tdc.jpg" is available in "jpg" format from:

<http://arxiv.org/ps/1503.07968v1>

This figure "7_adc.jpg" is available in "jpg" format from:

<http://arxiv.org/ps/1503.07968v1>

This figure "8_CH2C.jpg" is available in "jpg" format from:

<http://arxiv.org/ps/1503.07968v1>

This figure "9_.jpg" is available in "jpg" format from:

<http://arxiv.org/ps/1503.07968v1>

This figure "9b.jpg" is available in "jpg" format from:

<http://arxiv.org/ps/1503.07968v1>